Two-loop QCD corrections to *C*-even bottomonium exclusive decays to double J/ψ

Yu-Dong Zhang,[1,*] Xiao-Wei Bai,[2,†] Feng Feng,[3,4,‡] Wen-Long Sang,[2,5,§] and Ming-Zhen Zhou[2,‖]

[1]*Institute of Particle Physics and Key Laboratory of Quark and Lepton Physics (MOE), Central China Normal University, Wuhan, Hubei 430079, China*

[2]*School of Physical Science and Technology, Southwest University, Chongqing 400700, China*

[3]*Institute of High Energy Physics and Theoretical Physics Center for Science Facilities, Chinese Academy of Sciences, Beijing 100049, China*

[4]*China University of Mining and Technology, Beijing 100083, China*

[5]*College of Physics, Chongqing University, Chongqing 401331, China*

(Received 23 October 2023; accepted 7 December 2023; published 27 December 2023)

In the framework of nonrelativistic QCD (NRQCD) factorization, we compute both the polarized and the unpolarized decay widths for the processes $\eta_b(\chi_{bJ}) \to J/\psi J/\psi$, accurate up to next-to-next-to-leading order (NNLO) in α_s. For the first time, we confirm that the NRQCD factorization does hold at NNLO for the process involving triple quarkonia. We find that the radiative corrections are considerable. In particular, for χ_{b2}, both the $\mathcal{O}(\alpha_s)$ and $\mathcal{O}(\alpha_s^2)$ corrections are sizable and negative, and both can significantly reduce the leading-order prediction. At NNLO, the branching fractions are 8.2×10^{-7}, 6.2×10^{-6}, 7.2×10^{-7}, and 2.7×10^{-6} for $\eta_b, \chi_{b0}, \chi_{b1}$, and χ_{b2} decay, respectively. Our theoretical predictions are consistent with the upper limits measured by the Belle Collaboration. Moreover, we investigate the dependence of the theoretical predictions on the ratio of the charm quark mass and the bottom quark mass—i.e., $r = m_c/m_b$. By fixing m_b and varying m_c from 1.25 to 1.9 GeV, we find that the branching fraction can change by factors of 2, 3, and 6 for η_b, χ_{b0}, and χ_{b1}, respectively. Although the branching fraction for χ_{b2} decreases with the increase of r at leading order and next-to-leading order, it is almost independent of r at NNLO. In the phenomenological analysis, with the integrated luminosity $\mathcal{L} = 100\ \text{fb}^{-1}$, we expect about $(5-10) \times 10^3$ $\eta_b(\chi_{bJ}) \to J/\psi J/\psi \to \ell\bar{\ell}\ell\bar{\ell}$ events to be produced at the Large Hadron Collider; thus, it might be helpful to search for these processes. On the other hand, there are fewer than 100 $\eta_b(\chi_{bJ}) \to J/\psi J/\psi$ signal events at the B Factory, so it seems that the experimental measurements on these channels are quite challenging based on the current dataset. Nevertheless, with the designed 50 ab^{-1} integrated luminosity at Belle 2, the observation prospects of $\eta_b(\chi_{bJ}) \to J/\psi J/\psi$ may be promising in the foreseeable future.

DOI: 10.1103/PhysRevD.108.114030

I. INTRODUCTION

The exclusive decay of a bottomonium into double charmonia provides an excellent testing ground to explore the interplay between perturbative and nonperturbative aspects of the QCD. These processes can be studied in the framework of nonrelativistic QCD (NRQCD) factorization formalism [1], which offers a systematic way to separate the short-distance effects and long-distance effects. The experimentalists have made many attempts to search for such processes. Based on enormous $\Upsilon(1S)$ and $\Upsilon(2S)$ events, the Belle Collaboration has measured the branching fraction for $\Upsilon(1S) \to J/\psi\chi_{c1}$ and has set the upper limits for the branching fractions of $\Upsilon(nS) \to J/\psi\eta_c$ and $\Upsilon(nS) \to J/\psi\chi_{c0,2}$ [2]. Besides this, the search for double charmonium decays of the P-wave spin-triplet bottomonium states was performed in [3]. Although no significant χ_{bJ} signal was observed, the upper limits for the branching fractions of $\chi_{bJ} \to J/\psi J/\psi$ were obtained [3].

To date, the processes of a bottomonium exclusive decay into double charmonia have been extensively studied on the theoretical side. For Υ decay, the process of $\Upsilon \to J/\psi\eta_c$ was first studied a long time ago by Jia [4] within the

*ydzhang@mails.ccnu.edu.cn
†xiaoweibai22@163.com
‡f.feng@outlook.com
§wlsang@swu.edu.cn
‖zhoumz@swu.edu.cn

framework of NRQCD. The rate of $\Upsilon \to J/\psi\chi_{cJ}$ was first computed in Ref. [5]. The relativistic corrections and radiative corrections to these processes were separately considered in Refs. [6,7]. For C-even bottomonium decay, due to kinematic constraint, the amplitude of $\eta_b \to J/\psi J/\psi$ disappears at the lowest order in heavy quark velocity and α_s. The relativistic corrections to the rate of $\eta_b \to J/\psi J/\psi$ were first calculated in [8]. In the same year, the next-to-leading-order (NLO) radiative corrections were carried out [9]. The process was restudied based on the light-cone (LC) approach [10]. In 2010, Sun *et al.* recomputed the NLO corrections to the rate of $\eta_b \to J/\psi J/\psi$ in NRQCD [11]. Moreover, they also calculated the higher twist effects in the LC formalism. For $\chi_{bJ} \to J/\psi J/\psi$, the decay rate was first computed by Braguta *et al.* in both NRQCD and LC formalism [12]. Later, the relativistic corrections in the charm quark velocity were carried out in Refs. [13,14], and the NLO radiative corrections were worked out in Ref. [15].

In recent years, technological advances have made it possible to calculate the higher-order QCD corrections to quarkonium production and decay—in particular, for the processes involving multiple quarkonia. The two-loop radiative corrections to the cross section of $e^+e^- \to J/\psi\eta_c$ at the B Factory were computed in Refs. [16,17]. In the last year, the two-loop corrections to $e^+e^- \to J/\psi\chi_{cJ}$ were obtained in Ref. [18]. With all the available radiative corrections lumped together, the theoretical results on the production cross sections of $J/\psi + \eta_c(\chi_{c0})$ agree with the experimental measurements, notwithstanding large uncertainties. Very recently, the very challenging two-loop radiative corrections to $e^+e^- \to J/\psi J/\psi$ were carried out [19]. With the measured J/ψ decay constant as input, which amounts to resumming a specific class of radiative and relativistic corrections to all orders, the perturbative corrections exhibit a decent convergence behavior. The two-loop corrections to the decay width of $\Upsilon \to \eta_c(\chi_{cJ})\gamma$ were evaluated in 2021 [20]. In addition, the two-loop corrections to $\Upsilon \to J/\psi\eta_c(\chi_{cJ})$ were worked out last year [7], where the QCD corrections notably mitigate the renormalization-scale dependence of the decay widths, and the theoretical predictions on the branching fraction of $\Upsilon \to J/\psi\chi_{c1}$ are well consistent with the Belle measurement [2]. Inspired by the success of the NRQCD, we calculate, in the current work, the $\mathcal{O}(\alpha_s^2)$ corrections to the processes $\eta_b(\chi_{bJ}) \to J/\psi J/\psi$, which can provide useful guidance for experimental measurement.

This paper is organized as follows: In Sec. II, we present the general formulas for the helicity amplitudes and (un)polarized decay widths of $\eta_b(\chi_{bJ}) \to J/\psi J/\psi$. In Sec. III, we factorize the helicity amplitudes by employing the NRQCD factorization. In Sec. IV, we describe the technicalities encountered in the calculation and present the results of the various short-distance coefficients up to NNLO in α_s. Section V is devoted to the phenomenological analysis and discussion. A brief summary is given in Sec. VI. In Appendix A, we present the explicit expressions of the eight helicity projectors. In Appendix B, the decay widths as well as the branching fractions at various level of accuracy are tabulated for different ratios of the charm quark mass and the bottom quark mass.

II. (UN)POLARIZED DECAY WIDTHS

It is convenient to apply the helicity amplitude formalism [21,22] to analyze the exclusive decay $H \to J/\psi J/\psi$, where H can be η_b or χ_{bJ}. We assign the magnetic number S_z of the decaying particle directly along the z axis, and θ denotes the polar angle between the z axis and the direction of the outgoing J/ψ. Let λ_1 and λ_2 represent the helicities of the two outgoing J/ψ particles. The differential rate of H decay into $J/\psi(\lambda_1) + J/\psi(\lambda_2)$ becomes

$$\frac{d\Gamma[H(S_z) \to J/\psi(\lambda_1)J/\psi(\lambda_2)]}{d\cos\theta} = \frac{|\mathbf{P}|}{16\pi m_H^2} |d^J_{S_z,\lambda_1-\lambda_2}(\theta)|^2 |A^H_{\lambda_1,\lambda_2}|^2, \tag{1}$$

where m_H represents the mass of H, and $\mathbf{P}$ denotes the spatial components of the J/ψ momentum. The magnitude of $\mathbf{P}$ is readily determined via

$$|\mathbf{P}| = \frac{\lambda^{1/2}(m_H^2, m_{J/\psi}^2, m_{J/\psi}^2)}{2m_H} = \sqrt{\frac{m_H^2}{4} - m_{J/\psi}^2}, \tag{2}$$

where the Källen function is defined via $\lambda(x,y,z) = x^2+y^2+z^2-2xy-2xz-2yz$. Note that angular momentum conservation constrains $|\lambda_1 - \lambda_2| \le J$; here, J is the spin of H. The angular distribution is fully dictated by the quantum numbers λ_1 and λ_2 through the Wigner function $d^J_{S_z,\lambda_1-\lambda_2}(\theta)$, and $A^H_{\lambda_1,\lambda_2}$ is the intended helicity amplitude that encapsulates all nontrivial strong interaction dynamics, which depends upon λ_1 and λ_2.

Integrating (1) over $\cos\theta$ (one should cover only the hemisphere of the solid angle, since two J/ψ particles are indistinguishable bosons) and averaging over all possible H polarizations, one obtains

$$\begin{aligned}\Gamma[H \to J/\psi(\lambda_1)J/\psi(\lambda_2)] &= \frac{|\mathbf{P}|}{16\pi m_H^2} |A^H_{\lambda_1,\lambda_2}|^2 \int_0^1 \frac{1}{2J+1} \sum_{S_z} |d^J_{S_z,\lambda_1-\lambda_2}(\theta)|^2 d\cos\theta \\ &= \frac{|\mathbf{P}|}{16\pi(2J+1)m_H^2} |A^H_{\lambda_1,\lambda_2}|^2. \end{aligned} \tag{3}$$

The helicity amplitudes are not independent. Due to the parity invariance [21], there are the following relations:

$$A^{\eta_b}_{\lambda_1,\lambda_2} = -A^{\eta_b}_{-\lambda_1,-\lambda_2}, \qquad A^{\chi_{bJ}}_{\lambda_1,\lambda_2} = (-1)^J A^{\chi_{bJ}}_{-\lambda_1,-\lambda_2}. \tag{4}$$

Moreover, we have

$$A^{\eta_b}_{\lambda_1,\lambda_2} = -A^{\eta_b}_{\lambda_2,\lambda_1}, \qquad A^{\chi_{bJ}}_{\lambda_1,\lambda_2} = (-1)^J A^{\chi_{bJ}}_{\lambda_2,\lambda_1} \tag{5}$$

for the two identical J/ψ's in the final state [21]. Thus, there is one independent helicity amplitude for η_b and χ_{b1} decay; there are two for χ_{b0}, and four for χ_{b2}.

It is straightforward to obtain the unpolarized decay rates for $H \to J/\psi J/\psi$ by summing over all the allowed helicity channels:

$$\Gamma(\eta_b \to J/\psi J/\psi) = \frac{|\mathbf{P}|}{16\pi m^2_{\eta_b}}(2|A^{\eta_b}_{1,1}|^2), \tag{6a}$$

$$\Gamma(\chi_{b0} \to J/\psi J/\psi) = \frac{|\mathbf{P}|}{16\pi m^2_{\chi_{b0}}}(2|A^{\chi_{b0}}_{1,1}|^2 + |A^{\chi_{b0}}_{0,0}|^2), \tag{6b}$$

$$\Gamma(\chi_{b1} \to J/\psi J/\psi) = \frac{|\mathbf{P}|}{48\pi m^2_{\chi_{b1}}}(4|A^{\chi_{b1}}_{1,0}|^2), \tag{6c}$$

$$\Gamma(\chi_{b2} \to J/\psi J/\psi) = \frac{|\mathbf{P}|}{80\pi m^2_{\chi_{b2}}}(2|A^{\chi_{b2}}_{1,-1}|^2 + 2|A^{\chi_{b2}}_{1,1}|^2 + 4|A^{\chi_{b2}}_{1,0}|^2 + |A^{\chi_{b2}}_{0,0}|^2). \tag{6d}$$

Finally, it is enlightening to analyze the asymptotic behavior of the helicity amplitudes. In the limit of $m_b \gg m_c$, $A^H_{\lambda_1,\lambda_2}$ satisfies

$$A^H_{\lambda_1,\lambda_2} \propto r^{2+|\lambda_1+\lambda_2|}, \tag{7}$$

where $r = \frac{m_c}{m_b}$. For each J/ψ production, it contributes one power of r in (7) originating from the large momentum transfer which is required for the charm-anticharm pair to form the J/ψ with small relative momentum. The other powers of r arise from the helicity selection rule in perturbative QCD [23,24].

III. NRQCD FACTORIZATION FOR THE HELICITY AMPLITUDE

By employing the NRQCD factorization [1], we can express the helicity amplitude as

$$A^H_{\lambda_1,\lambda_2} = \sqrt{2m_H}2m_{J/\psi} f^H_{\lambda_1,\lambda_2} \frac{\sqrt{\langle\mathcal{O}\rangle_H}}{m_b^n} \frac{\langle\mathcal{O}\rangle_{J/\psi}}{m_c^3}, \tag{8}$$

where $n = 2$ for η_b and $n = 3$ for χ_{bJ}, and $f^H_{\lambda_1,\lambda_2}$ denotes the dimensionless short-distance coefficient (SDC). The nonperturbative long-distance matrix element (LDME) is defined via $\langle\mathcal{O}\rangle_H \equiv |\langle 0|\mathcal{O}_H|H\rangle|^2$ with

$$\mathcal{O}_{\eta_b} = \chi^\dagger\psi, \tag{9a}$$

$$\mathcal{O}_{\chi_{b0}} = \frac{1}{\sqrt{3}}\chi^\dagger\left(-\frac{i}{2}\overleftrightarrow{\mathbf{D}}\cdot\boldsymbol{\sigma}\right)\psi, \tag{9b}$$

$$\mathcal{O}_{\chi_{b1}} = \frac{1}{\sqrt{2}}\chi^\dagger\left(-\frac{i}{2}\overleftrightarrow{\boldsymbol{D}}\times\boldsymbol{\sigma}\right)\cdot\boldsymbol{\epsilon}_{\chi_{b1}}\psi, \tag{9c}$$

$$\mathcal{O}_{\chi_{b2}} = \chi^\dagger\left(-\frac{i}{2}\overleftrightarrow{D}^{(i}\sigma^{j)}\right)\epsilon^{ij}_{\chi_{b2}}\psi, \tag{9d}$$

$$\mathcal{O}_{J/\psi} = \chi^\dagger\boldsymbol{\sigma}\cdot\boldsymbol{\epsilon}_{J/\psi}\psi, \tag{9e}$$

where ψ and $\chi^\dagger$ are the Pauli spinor fields annihilating a heavy quark and antiquark, respectively, and ϵ_H and $\epsilon_{J/\psi}$ represent the polarization tensor/vector of H and J/ψ, respectively.

The prefactor $\sqrt{2m_H}2m_{J/\psi}$ in (8) originates from the fact that we adopt relativistic normalization for the quarkonium in the helicity amplitude; however, we adopt nonrelativistic normalization in the LDMEs. Since, in this work, we are only concerned with the lowest order in velocity expansion, we can set $m_H = 2m_b$ and $m_{J/\psi} = 2m_c$ in (8).

It is worth noting that the helicity selection rule for SDCs,

$$f^H_{\lambda_1,\lambda_2} \propto r^{1+|\lambda_1+\lambda_2|}, \tag{10}$$

can be directly deduced from (7) by noticing that $\langle\mathcal{O}\rangle_{J/\psi} \propto m_c^3$.

It is convenient to expand the helicity SDCs in powers of the strong coupling constant

$$\begin{aligned} f^H_{\lambda_1,\lambda_2} = \alpha_s^2\Bigg[& f^{H,(0)}_{\lambda_1,\lambda_2} + \frac{\alpha_s}{\pi}\left(\frac{\beta_0}{2}\ln\frac{\mu_R^2}{m_b^2} f^{H,(0)}_{\lambda_1,\lambda_2} + f^{H,(1)}_{\lambda_1,\lambda_2}\right) \\ & + \frac{\alpha_s^2}{\pi^2}\left(\frac{3\beta_0^2}{16}\ln^2\frac{\mu_R^2}{m_b^2} f^{H,(0)}_{\lambda_1,\lambda_2}\right. \\ & + \left(\frac{\beta_1}{8} f^{H,(0)}_{\lambda_1,\lambda_2} + \frac{3\beta_0}{4} f^{H,(1)}_{\lambda_1,\lambda_2}\right)\ln\frac{\mu_R^2}{m_b^2} \\ & \left. + (2\gamma_{J/\psi} + \gamma_H)\ln\frac{\mu_\Lambda^2}{m_c^2} f^{H,(0)}_{\lambda_1,\lambda_2} + f^{H,(2)}_{\lambda_1,\lambda_2}\right)\Bigg] + \mathcal{O}(\alpha_s^5), \end{aligned} \tag{11}$$

where $\beta_0 = \frac{11}{3}C_A - \frac{4}{3}T_F n_f$ and $\beta_1 = \frac{34}{3}C_A^2 - (\frac{20}{3}C_A + 4C_F)T_F n_f$ are the one-loop and two-loop coefficients of the QCD β function, respectively, and $n_f = n_L + n_H$ signifies the number of active flavors, with the number of light quarks being $n_L = 3$, and the number of heavy quarks $n_H = 1$. μ_R and μ_Λ refer to the renormalization scale and the NRQCD factorization scale, respectively. The $\ln\mu_R^2$ terms in (11) guarantee the renormalization group invariance of the SDCs. The occurrence of $\ln\mu_\Lambda^2$ is required by the NRQCD factorization. According to the factorization, the μ_Λ dependence in the SDCs should be thoroughly eliminated by that in the LDMEs. $\gamma_{J/\psi}$ and γ_H represent the anomalous dimensions associated with the NRQCD

bilinear currents carrying the quantum numbers $^3S_1$, $^1S_0$, or ^3P_J, which have already been known from various sources [25–30]:

$$\gamma_{J/\psi} = -\pi^2\left(\frac{C_A C_F}{4} + \frac{C_F^2}{6}\right), \tag{12a}$$

$$\gamma_{\eta_b} = -\pi^2\left(\frac{C_A C_F}{4} + \frac{C_F^2}{2}\right), \tag{12b}$$

$$\gamma_{\chi_{b0}} = -\pi^2\left(\frac{C_A C_F}{12} + \frac{C_F^2}{3}\right), \tag{12c}$$

$$\gamma_{\chi_{b1}} = -\pi^2\left(\frac{C_A C_F}{12} + \frac{5C_F^2}{24}\right), \tag{12d}$$

$$\gamma_{\chi_{b2}} = -\pi^2\left(\frac{C_A C_F}{12} + \frac{13C_F^2}{120}\right). \tag{12e}$$

The SDCs can be determined by the perturbative matching procedure—i.e., by replacing the physical $J/\psi/H$ with the fictitious quarkonia composed of the free $c\bar{c}/b\bar{b}$ pair with the same quantum numbers as $J/\psi/H$, computing both sides in (8) in perturbative QCD and NRQCD, then solving for SDCs order by order in perturbation theory.

IV. SDCs UP TO NNLO

We employ the FeynArts package [31] to generate the quark-level Feynman diagrams and Feynman amplitudes for $b\bar{b} \to c\bar{c} + c\bar{c}$. Some representative Feynman diagrams are illustrated in Fig. 1. We adopt the well-known covariant color/spin/orbital projector technique with the aid of the packages FeynCalc [32] and FormLink [33] to expedite the matching calculation. To further extract the helicity amplitudes, we find it convenient to apply various covariant helicity projectors. The expressions of these helicity projectors are explicitly presented in Appendix A.

It is straightforward to compute the leading-order (LO) SDCs

$$f_{1,1}^{\chi_{b0},(0)} = \frac{64\sqrt{3}\pi^2 r^3}{81}, \qquad f_{0,0}^{\chi_{b0},(0)} = -\frac{32\sqrt{3}\pi^2 r(1-2r^2)}{81}, \tag{13a}$$

$$f_{1,1}^{\chi_{b2},(0)} = -\frac{64\sqrt{6}\pi^2 r^3}{81}, \quad f_{1,0}^{\chi_{b2},(0)} = \frac{32\sqrt{2}\pi^2 r^2}{27}, \tag{13b}$$

$$f_{1,-1}^{\chi_{b2},(0)} = -\frac{32\pi^2 r}{27}, \qquad f_{0,0}^{\chi_{b2},(0)} = -\frac{16\sqrt{6}\pi^2 r(1+4r^2)}{81}, \tag{13c}$$

which are consistent with those in Refs. [9,11,13]. Accidentally, we find that the SDCs for η_b and χ_{b1} vanish at LO. This can be explained by the following fact: At LO, the amplitude of the subprocess $\eta_b(\chi_{b1}) \to g^* g^*$ is proportional to a Levi-Civita tensor, and by coincidence, the momenta of the two virtual gluons are equal, which cause the Levi-Civita tensor to vanish. In addition, it is straightforward to check that the value $f^{H,(0)}$ in (13) satisfy the helicity scaling rule (10) in the limit of $r \to 0$.

Once beyond the LO, we adopt the standard shortcut to directly extract the SDCs—i.e., to expand the QCD amplitudes in powers of quark relative momentum prior to conducting loop integrals, which amounts to directly extracting the contribution from the hard region in the context of strategy of region [34]. We utilize the packages Apart [35] and FIRE [36] to reduce the loop integrals into linear combinations of a group of master integrals (MIs). Finally, we end up with 20 one-loop MIs, which are analytically computed with the aid of Package-X [37], and 1439 two-loop MIs, which are numerically evaluated with the method of auxiliary mass flow [38–41]. Moreover, we employ the newly released package

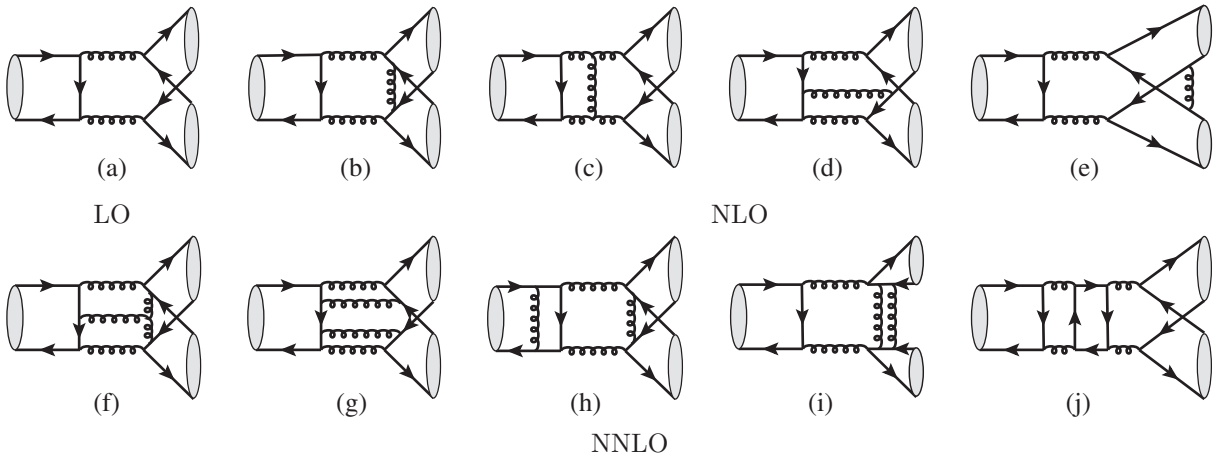

FIG. 1. Some representative Feynman diagrams for the process $H \to J/\psi J/\psi$ up to two loops.

CalcLoop [42], developed by Ma *et al.*, to check some of our computation.

Performing the field-strength and mass renormalization, with two-loop expressions of Z_2 and Z_m taken from [43], and renormalizing the strong coupling constant under the $\overline{\rm MS}$ scheme to two-loop order, we eliminate the UV divergences in the two-loop SDCs. Nevertheless, the renormalized two-loop corrections to the SDCs still contain uncanceled single IR poles. This pattern is exactly what is required by NRQCD factorization, as reflected in (11). These IR poles can be factored into the NRQCD LDMEs under the $\overline{\rm MS}$ prescription, which then become scale-dependent quantities. As mentioned previously, the $\ln\mu_\Lambda$ terms in (11) exactly cancel the μ_Λ dependence of the LDMEs, so that the predicted decay width is independent of μ_Λ. The validity of NRQCD factorization in this process turns out to be highly nontrivial.

Since the analytic expressions of the $f^{H,(1)}_{\lambda_1,\lambda_2}$ are too complicated, here we merely present their asymptotic expansion in the limit of $r\to 0$:

$$f^{H,(1)}_{\lambda_1,\lambda_2}\Big|_{\rm asy}=\frac{64\pi^2}{81}r^{1+|\lambda_1+\lambda_2|}\mathcal{C}^H_{\lambda_1,\lambda_2}, \tag{14}$$

where we have deliberately pulled out the r-dependent factor in front to make the helicity scaling rule manifest, so that the $\mathcal{C}^H_{\lambda_1,\lambda_2}$ values scale as r^0 and read

$$\mathcal{C}^{\eta_b}_{1,1}=\frac{19\ln^2 r}{8}+\left(\frac{5}{2}+\frac{19i\pi}{8}-\frac{\ln 2}{4}\right)\ln r+\frac{5\ln^2 2}{16}+\left(\frac{1}{2}+\frac{i\pi}{8}\right)\ln 2+\frac{29\pi^2}{96}-\frac{3\sqrt{3}\pi}{8}+i\pi+\frac{3}{4}, \tag{15a}$$

$$\mathcal{C}^{\chi_{b0}}_{1,1}=-\frac{59\ln^2 r}{8\sqrt{3}}+\sqrt{3}\left(\frac{25\ln 2}{12}-\frac{22}{3}-\frac{59i\pi}{24}\right)\ln r+\frac{25\sqrt{3}}{16}\ln^2 2-\sqrt{3}\left(\frac{11}{2}+\frac{33i\pi}{8}\right)\ln 2+\sqrt{3}\left(\frac{983}{144}+\frac{65i\pi}{24}-\frac{19\pi^2}{32}\right)$$
$$+\frac{\pi}{3}-\frac{\sqrt{3}n_f}{9}(3i\pi+5), \tag{15b}$$

$$\mathcal{C}^{\chi_{b0}}_{0,0}=\frac{(15-10\ln 2)\sqrt{3}}{6}\ln r-\sqrt{3}\left(\frac{1}{2}+\frac{13i\pi}{24}\right)\ln 2+\sqrt{3}\left(\frac{17\pi^2}{96}-\frac{511}{144}-\frac{25i\pi}{24}\right)+\frac{\sqrt{3}}{4}\ln^2 2+\frac{37\pi}{48}+\frac{\sqrt{3}n_f}{18}(3i\pi+5), \tag{15c}$$

$$\mathcal{C}^{\chi_{b1}}_{1,0}=\frac{\ln^2 r}{8\sqrt{2}}+\sqrt{2}\left(\frac{5\ln 2}{8}-\frac{7}{64}+\frac{i\pi}{16}\right)\ln r-\frac{97\ln^2 2}{8\sqrt{2}}+\sqrt{2}\left(\frac{159}{16}+\frac{51i\pi}{4}\right)\ln 2+\sqrt{2}\left(\frac{13\pi^2}{96}-\frac{583}{256}-\frac{127i\pi}{16}-\frac{21\sqrt{3}\pi}{32}\right), \tag{15d}$$

$$\mathcal{C}^{\chi_{b2}}_{1,1}=\frac{13\ln^2 r}{2\sqrt{6}}-\sqrt{6}\left(\frac{37\ln 2}{12}-\frac{29}{6}-\frac{13i\pi}{12}\right)\ln r+\frac{411\sqrt{6}}{16}\ln^2 2-\sqrt{6}\left(\frac{1123}{30}+52i\pi\right)\ln 2+\sqrt{6}\left(\frac{3851}{720}+\frac{731i\pi}{20}+\frac{29\pi^2}{96}\right)$$
$$+\frac{1261\pi}{120\sqrt{2}}+\frac{\sqrt{6}n_f}{9}(3i\pi+5), \tag{15e}$$

$$\mathcal{C}^{\chi_{b2}}_{1,0}=-\frac{17\ln^2 r}{8\sqrt{2}}+\sqrt{2}\left(\frac{21\ln 2}{8}-\frac{335}{64}-\frac{17i\pi}{16}\right)\ln r+\frac{417\ln^2 2}{8\sqrt{2}}-\sqrt{2}\left(\frac{8879}{240}+\frac{857i\pi}{16}\right)\ln 2$$
$$+\sqrt{2}\left(\frac{76087}{3840}+\frac{17779i\pi}{480}-\frac{67\pi^2}{64}\right)-\frac{181\sqrt{6}\pi}{480}-\frac{\sqrt{2}n_f}{6}(3i\pi+5), \tag{15f}$$

$$\mathcal{C}^{\chi_{b2}}_{1,-1}=(6-8\ln 2)\ln r+10\ln^2 2-\left(\frac{453}{20}+\frac{163i\pi}{8}\right)\ln 2+\frac{73\pi^2}{96}+\frac{5801i\pi}{480}-\frac{1157}{240}+\frac{1081\sqrt{3}\pi}{480}+\frac{n_f}{6}(3i\pi+5), \tag{15g}$$

$$\mathcal{C}^{\chi_{b2}}_{0,0}=\frac{(3-2\ln 2)\sqrt{6}}{6}\ln r+\frac{13\sqrt{6}}{4}\ln^2 2-\sqrt{6}\left(\frac{259}{60}+\frac{161i\pi}{24}\right)\ln 2-\sqrt{6}\left(\frac{1067}{1440}-\frac{2141i\pi}{480}+\frac{\pi^2}{32}\right)$$
$$+\frac{197\sqrt{2}\pi}{120}+\frac{\sqrt{6}n_f}{36}(3i\pi+5). \tag{15h}$$

It is worth noting that the above asymptotic expressions can hardly approximate the complete expressions for most $f^{(1)}_{\lambda_1,\lambda_2}$ cases at physical values of m_c and m_b, due to m_b being far from asymptotically larger than m_c.

TABLE I. Numerical values for various SDCs with $m_b = 4.7$ GeV and $m_c = 1.5$ GeV.

$m_c = 1.50$ GeV, $m_b = 4.70$ GeV				
H	(λ_1, λ_2)	$f^{(0)}_{\lambda_1,\lambda_2}$	$f^{(1)}_{\lambda_1,\lambda_2}$	$f^{(2)}_{\lambda_1,\lambda_2}$
η_b	(1,1)	$\cdots$	$0.551 - 1.410i$	$21.624 - 10.293i$
χ_{b0}	(1,1)	0.439	$-0.266 + 2.726i$	$-86.938 + 29.858i$
	(0,0)	-1.716	$-2.830 - 6.283i$	$184.697 - 75.742i$
χ_{b1}	(1,0)	$\cdots$	$-0.281 + 1.188i$	$8.812 + 7.876i$
χ_{b2}	(1,1)	-0.621	$3.801 + 0.233i$	$84.482 - 2.120i$
	(1,0)	1.685	$-9.666 - 1.178i$	$-221.561 - 1.457i$
	(1, −1)	-3.733	$21.499 + 2.214i$	$465.006 + 10.900i$
	(0,0)	-2.145	$11.326 + 2.567i$	$278.731 + 3.346i$

Finally, we identify the desired nonlogarithmic piece in the two-loop SDCs. It becomes much more challenging to deduce the analytical expressions for the encountered two-loop MIs. Instead, we resort to the high-precision numerical computation. By taking the bottom quark and charm quark pole masses to the typical values $m_b = 4.70$ GeV and $m_c = 1.50$ GeV, respectively, we tabulate the results of $f^{H,(2)}_{\lambda_1,\lambda_2}$ in Table I. For completeness, the numerical values of $f^{H,(0)}_{\lambda_1,\lambda_2}$ and $f^{H,(1)}_{\lambda_1,\lambda_2}$ are also listed.

V. PHENOMENOLOGY AND DISCUSSION

Prior to making phenomenological predictions, we specify our choice of the various input parameters. In order to reduce the theoretical uncertainty, we use the physical quarkonium masses in computing the phase space in (6). But beyond that, we choose $m_H = 2m_b$ and $m_{J/\psi} = 2m_c$ so as to maintain gauge invariance. The physical quarkonium masses are taken from the particle data group (PDG) [44]: $m_{\eta_b} = 9.3987$ GeV, $m_{\chi_{b0}} = 9.85944$ GeV, $m_{\chi_{b1}} = 9.89278$ GeV, $m_{\chi_{b2}} = 9.91221$ GeV, and $m_{J/\psi} = 3.0969$ GeV. We choose the benchmark values of the heavy quark pole masses, $m_b = 4.7$ GeV and $m_c = 1.5$ GeV. In addition, we will investigate the dependence of the theoretical results on the mass ratio r.

We approximate the NRQCD LDMEs at $\mu_\Lambda = 1$ GeV by the Schrödinger radial wave function at the origin and the first derivative of the Schrödinger radial wave function at the origin for the S-wave and P-wave quarkonia, respectively:

$$\langle \mathcal{O} \rangle_{J/\psi} \approx \frac{N_c}{2\pi} |R^{c\bar{c}}_{1S}(0)|^2 = \frac{N_c}{2\pi} \times 0.810 \text{ GeV}^3, \tag{16a}$$

$$\langle \mathcal{O} \rangle_{\eta_b} \approx \frac{N_c}{2\pi} |R^{b\bar{b}}_{1S}(0)|^2 = \frac{N_c}{2\pi} \times 6.477 \text{ GeV}^3, \tag{16b}$$

$$\langle \mathcal{O} \rangle_{\chi_{bJ}} \approx \frac{3N_c}{2\pi} |R'^{b\bar{b}}_{1P}(0)|^2 = \frac{3N_c}{2\pi} \times 1.417 \text{ GeV}^5, \tag{16c}$$

TABLE II. Total decay widths of χ_{bJ}.

H	$\Gamma[\chi_{bJ} \to \gamma\Upsilon]$(keV) [47]	$\text{Br}[\chi_{bJ} \to \gamma\Upsilon]$ [44]	Γ_{tot}(MeV)
χ_{b0}	22.2	$(1.94 \pm 0.27)\%$	$1.144^{+0.185}_{-0.140}$
χ_{b1}	27.8	$(35.2 \pm 2.0)\%$	$0.079^{+0.005}_{-0.004}$
χ_{b2}	31.6	$(18.0 \pm 1.0)\%$	$0.176^{+0.010}_{-0.009}$

where the radial wave functions at the origin are evaluated from the Buchmüller-Tye (BT) potential model [45]. Note that we have made the approximation $\langle \mathcal{O} \rangle_{\chi_{b0}} \approx \langle \mathcal{O} \rangle_{\chi_{b1}} \approx \langle \mathcal{O} \rangle_{\chi_{b2}}$ by invoking the heavy quark spin symmetry.

We fix $\mu_\Lambda = 1$ GeV. The central value of μ_R is chosen, $\mu_R = m_b$, and we vary μ_R from $2m_c$ to $2m_b$ to estimate the theoretical uncertainties. The QCD running coupling constant is evaluated with the aid of the package RunDec [46] at two loops.

To further predict the branching fractions of various decay channels, we need to specify the total decay widths of η_b and χ_{bJ}. The decay width of η_b can be directly taken from the PDG [44]: $\Gamma_{\eta_b} = 10^{+5}_{-4}$ MeV. So far, the decay widths of χ_{bJ} are absent from the PDG. Nevertheless, we can determine the decay widths of χ_{bJ} through

$$\Gamma_{\text{tot}}(\chi_{bJ}) = \frac{\Gamma[\chi_{bJ} \to \gamma\Upsilon]}{\text{Br}[\chi_{bJ} \to \gamma\Upsilon]}, \tag{17}$$

where the branching fractions of the E1 transition are measured [44], and the decay widths of the E1 transition have been given in Ref. [47]. We enumerate all the results in Table II, where the uncertainty in Γ_{tot} originates from $\text{Br}[\chi_{bJ} \to \gamma\Upsilon]$.

Now, we collect all the ingredients to perform phenomenological analysis. In Table III, we tabulate the theoretical predictions on the (un)polarized decay widths and the branching fractions at various levels of accuracy in α_s. To facilitate comparison, the upper limits of various channels from the Belle measurements [3] are listed in the last column. The uncertainty affiliated with the decay width is caused by sliding the renormalization scale μ_R, and the two uncertainties in the branching fraction are from the renormalization scale and total decay width. We should emphasize that there are other sources of uncertainties for the theoretical predictions—e.g., the values of the Schrödinger wave functions and the uncalculated relativistic corrections, which may potentially bring about extra uncertainties. In addition, we do not include the contributions from the Feynman diagrams where the double J/ψ's are produced through two virtual photon independent fragmentations, which actually are much less than the nonfragmentation contributions [8,9,13,48], and therefore can be safely neglected. It is worth noting that the situation is quite different from the process $e^+e^- \to J/\psi J/\psi$, where the dominant production mechanism is via two photon independent fragmentations into J/ψ.

TABLE III. Theoretical predictions on various (un)polarized decay widths (in units of eV) and branching fractions ($\times 10^{-5}$). The uncertainties affiliated with the decay widths are estimated by varying μ_R from $2m_c$ to $2m_b$, with the central values evaluated at $\mu_R = m_b$. The two uncertainties in the branching fraction are from the renormalization scale μ_R and the total decay widths of η_b/χ_{bJ}, respectively.

H	Order	$\Gamma_{0,0}$	$\Gamma_{1,0}$	$\Gamma_{1,1}$	$\Gamma_{1,-1}$	$\Gamma_{\rm Unpol}$	$\mathrm{Br}_{\rm th}$	$\mathrm{Br}_{\rm exp}$ [3]
η_b	LO	…	…	…	…	…	…	…
	NLO	…	…	$1.080^{+1.663}_{-0.714}$	…	$2.160^{+3.325}_{-1.428}$	$0.022^{+0.033+0.014}_{-0.014-0.007}$	
	NNLO	…	…	$4.084^{+3.987}_{-2.232}$	…	$8.168^{+7.973}_{-4.463}$	$0.082^{+0.080+0.054}_{-0.045-0.027}$	
χ_{b0}	LO	$8.542^{+7.358}_{-4.393}$	…	$0.559^{+0.482}_{-0.288}$	…	$9.660^{+8.321}_{-4.968}$	$0.844^{+0.727+0.117}_{-0.434-0.118}$	< 7.1
	NLO	$11.140^{+1.233}_{-2.500}$	…	$0.616^{+0.084}_{-0.124}$	…	$12.372^{+1.400}_{-2.748}$	$1.081^{+0.122+0.150}_{-0.240-0.151}$	
	NNLO	$6.449^{+1.710}_{-1.955}$	…	$0.329^{+0.371}_{-0.012}$	…	$7.107^{+1.741}_{-1.212}$	$0.621^{+0.152+0.086}_{-0.106-0.086}$	
χ_{b1}	LO	…	…	…	…	…	…	< 2.7
	NLO	…	$0.007^{+0.011}_{-0.005}$	…	…	$0.027^{+0.042}_{-0.018}$	$0.035^{+0.053+0.002}_{-0.023-0.002}$	
	NNLO	…	$0.014^{+0.009}_{-0.006}$	…	…	$0.057^{+0.035}_{-0.026}$	$0.072^{+0.044+0.004}_{-0.033-0.004}$	
χ_{b2}	LO	$2.663^{+2.294}_{-1.370}$	$1.643^{+1.416}_{-0.845}$	$0.223^{+0.192}_{-0.115}$	$8.067^{+6.949}_{-4.149}$	$25.818^{+22.239}_{-13.279}$	$14.669^{+12.636+0.884}_{-7.545-0.789}$	< 4.5
	NLO	$1.094^{+0.281}_{-0.679}$	$0.604^{+0.199}_{-0.423}$	$0.075^{+0.030}_{-0.057}$	$2.943^{+0.987}_{-2.084}$	$9.545^{+3.111}_{-6.655}$	$5.424^{+1.768+0.327}_{-3.781-0.292}$	
	NNLO	$0.071^{+0.476}_{-0.048}$	$0.020^{+0.267}_{-0.015}$	$0.001^{+0.032}_{-0.001}$	$0.157^{+1.351}_{-0.130}$	$0.467^{+4.311}_{-0.360}$	$0.265^{+2.450+0.016}_{-0.205-0.014}$	

Examining Table III closely, we find that the polarized decay widths roughly obey the hierarchy as indicated by the helicity scaling rule in (7). It is interesting to note that both the NLO and NNLO perturbative corrections to $\Gamma[\chi_{b2} \to J/\psi J/\psi]$ are sizable and negative. Incorporating the perturbative corrections significantly reduces the LO prediction, which indicates that the perturbative convergence is rather poor. Because of this, the theoretical

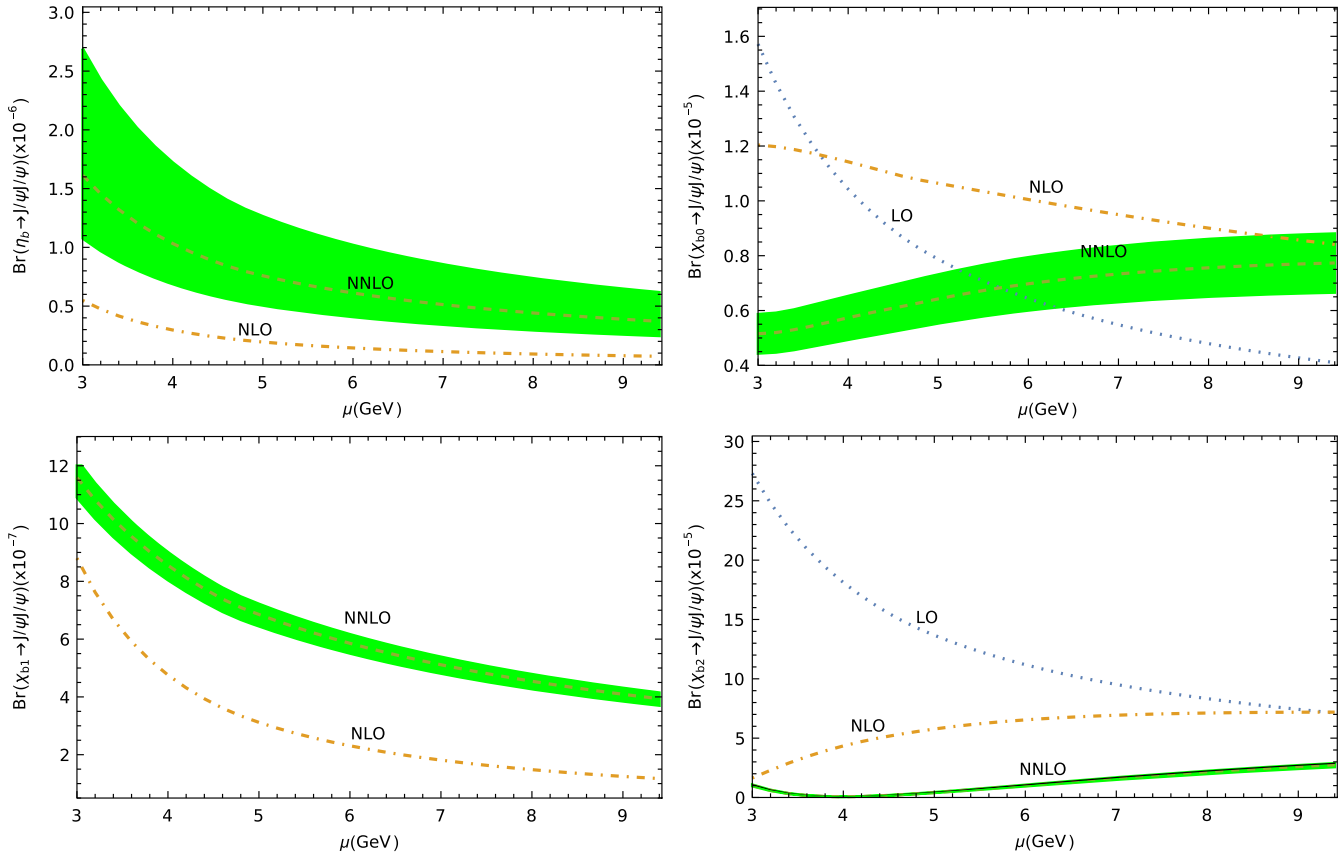

FIG. 2. Theoretical predictions for $\mathrm{Br}[\eta_b(\chi_{bJ}) \to J/\psi J/\psi]$ as a function of μ_R at various levels of accuracy in α_s.

prediction bears large μ_R dependence for χ_{b2}. In addition, the decay widths of η_b and χ_{b1} are much smaller than those of the other two channels, which is attributed to the vanishing LO amplitudes for η_b and χ_{b1}. Finally, we find that the theoretical predictions on the branching fractions are consistent with the upper limits measured by the Belle Collaboration [3].

In Fig. 2, we plot the branching fractions as a function of the renormalization scale μ_R at various levels of perturbative accuracy. The green band corresponds to the uncertainty affiliated with the total decay widths of η_b and χ_{bJ}. We observe that the perturbative corrections seem to considerably reduce the LO μ_R dependence for χ_{b0} and slightly reduce the μ_R dependence for χ_{b1}, but they worsen the μ_R dependence for η_b.

It is instructive to further investigate the dependence of the theoretical predictions on the mass ratio r. By fixing LDMEs, $\mu_R = m_b$ and $m_b = 4.7$ GeV, and varying m_c from 1.25 GeV to 1.9 GeV, we plot the branching fractions as a function of r at various levels of accuracy in α_s in Fig. 3. We observe that the branching fractions monotonically decrease as r increases for η_b and $\chi_{b0,1}$ at every perturbative accuracy. By analyzing the data in Appendix B, we find that, by varying m_c from 1.25 GeV to 1.9 GeV, the branching fractions roughly change by a factor of 2, 3, and 6 for η_b, χ_{b0}, and χ_{b1}, respectively. Although the branching fraction for χ_{b2} decreases with the increase of r both at LO and at NLO, the branching fraction at NNLO is almost independent of r.

Finally, we utilize the results in Table III to estimate the observing prospects at the LHC and B Factory. The production cross sections for χ_{b0} and χ_{b2} at the LHC at $\sqrt{s} = 14$ TeV are evaluated: $\sigma(\mathrm{pp} \to \chi_{b0} + \mathrm{X}) = 1.5\ \mu\mathrm{b}$, and $\sigma(\mathrm{pp} \to \chi_{b2} + \mathrm{X}) = 2.0\ \mu\mathrm{b}$ [49]. The cross section for η_b production is roughly estimated to be $\sigma(\mathrm{pp} \to \eta_b + \mathrm{X}) = 15\,\mu\mathrm{b}$ [8]. If we take the integrated luminosity $\mathcal{L} = 100\ \mathrm{fb}^{-1}$, it is expected that there will be about 10^6 exclusive double J/ψ events from η_b and χ_{b0} decay, and 5×10^5 from χ_{b2} decay at the LHC. Furthermore, taking into account $\mathrm{Br}[J/\psi \to \ell\bar{\ell}] = 12\%$, about $(5-10) \times 10^3$ four-lepton events from double J/ψ can be produced. Although there are potentially copious double J/ψ background events, it might be helpful to establish the $\eta_b(\chi_{bJ}) \to J/\psi J/\psi$ signals. At the B Factory, η_b and χ_{bJ} can be produced through $\Upsilon(2S)$ electromagnetic E1 transition. Using a sample of $158 \times 10^6 \Upsilon(2S)$ events collected by the Belle detector, we expect about 10^5 η_b and 6×10^6 χ_{b0}, and 10^7 $\chi_{b1,2}$ events can be accumulated. Consequently, it is estimated that there are fewer than 100 double J/ψ events. So, the experimental measurements on these channels are challenging based on the current dataset

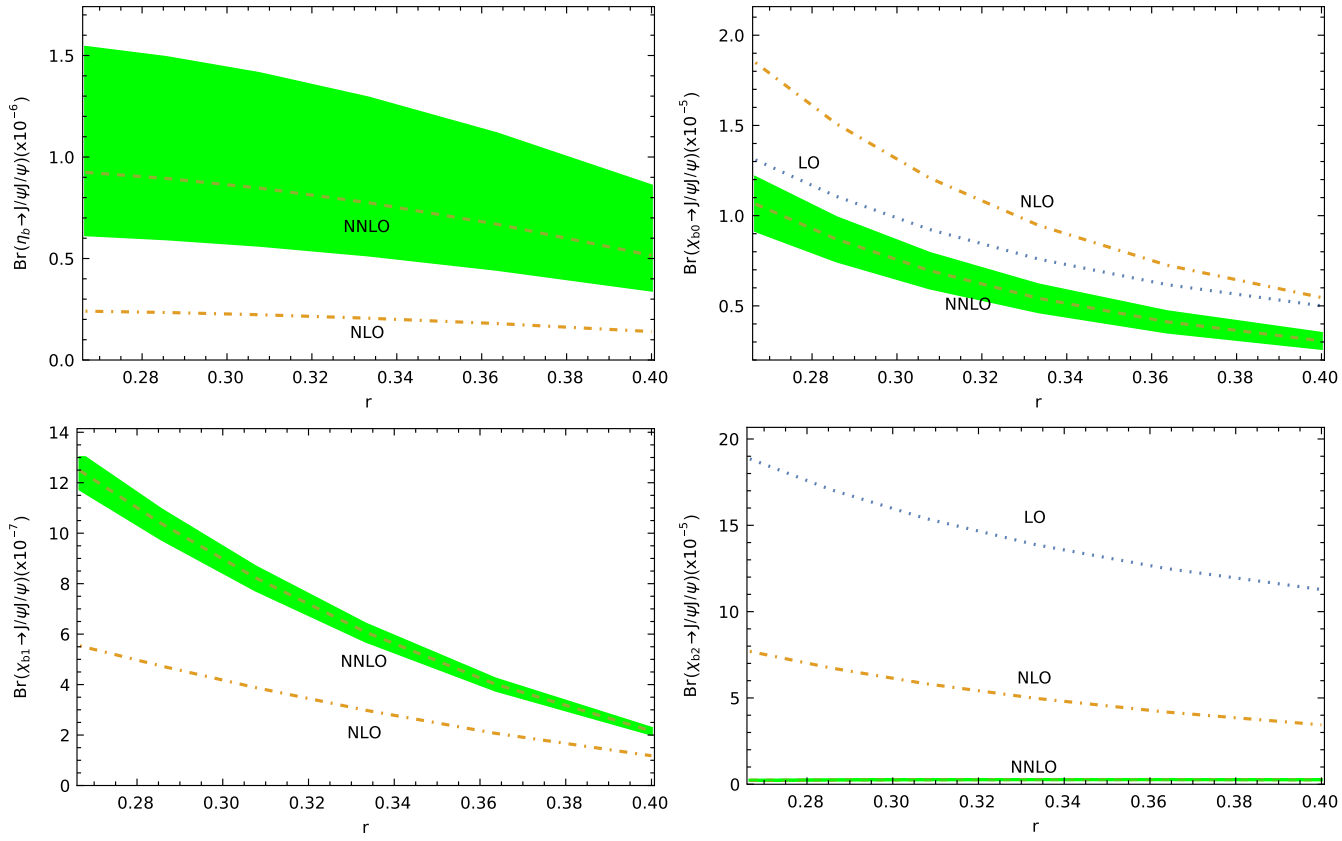

FIG. 3. Branching fractions of $\eta_b(\chi_{bJ}) \to J/\psi J/\psi$ as a function of r.

at the B Factory. Nevertheless, with the designed 50 ab^{-1} integrated luminosity at Belle 2, it seems that the observation prospects of $\eta_b(\chi_{bJ}) \to J/\psi J/\psi$ are promising in the foreseeable future.

VI. SUMMARY

Based on the NRQCD factorization, we compute both the polarized and the unpolarized decay widths for the processes $\eta_b(\chi_{bJ}) \to J/\psi J/\psi$ up to NNLO in α_s. By taking the decay width of η_b from PDG and determining the total decay widths of χ_{bJ} through their electromagnetic E1 transition into Υ, we also predict the branching fractions for $\eta_b(\chi_{bJ}) \to J/\psi J/\psi$. We find that the perturbative corrections are sizable for η_b and χ_{b2} decay. In particular, for χ_{b2}, both the $\mathcal{O}(\alpha_s)$ and $\mathcal{O}(\alpha_s^2)$ corrections can significantly reduce the LO prediction. Moreover, we observe that the decay widths for η_b and χ_{b1} are much smaller than those of the other two channels, which can be attributed to the vanishing LO amplitudes for η_b and χ_{b1}. By including all the radiative corrections, we find that the branching fractions are 8.2×10^{-7}, 6.2×10^{-6}, 7.2×10^{-7}, and 2.7×10^{-6} for η_b, χ_{b0}, χ_{b1}, and χ_{b2}, respectively. Our theoretical predictions are consistent with the upper limits measured by the Belle Collaboration.

We also investigate the dependence of the theoretical predictions on the mass ratio r. By fixing m_b and the LDMEs, and varying r from 0.26 to 0.4, we find that the branching fraction can change by a factor of 2, 3, and 6 for η_b, χ_{b0}, and χ_{b1}, respectively. Although the branching fraction for χ_{b2} decreases with the increase of r at LO and NLO, it is almost independent of r at NNLO.

Finally, we explore the observing prospects for $\eta_b(\chi_{bJ}) \to J/\psi J/\psi$ at the LHC and B Factory. We expect that there are about $(5-10) \times 10^5$ double J/ψ signal events produced at the LHC, and fewer than 100 events at the B Factory. Taking into account $\mathrm{Br}[J/\psi \to \ell\bar{\ell}] = 12\%$, several thousands of four-lepton events from double J/ψ can be produced at the LHC. If a copious double J/ψ background can be well separated, the experimental measurements on $\eta_b(\chi_{bJ}) \to J/\psi J/\psi$ might be helpful at the LHC. The measurement on $\eta_b(\chi_{bJ}) \to J/\psi J/\psi$ at the B Factory is quite challenging based on the current dataset. Nevertheless, with the designed 50 ab^{-1} integrated luminosity at Belle 2, the observation prospects for $\eta_b(\chi_{bJ}) \to J/\psi J/\psi$ may be promising in the foreseeable future.

ACKNOWLEDGMENTS

The work of Y.-D. Z. is supported by the National Natural Science Foundation of China under Grants No. 12135006 and No. 12075097, and by the Fundamental Research Funds for the Central Universities under Grants No. CCNU20TS007 and No. CCNU22LJ004. The work of X.-W. B., W.-L. S., and M.-Z. Z. is supported by the National Natural Science Foundation of China under Grants No. 12375079 and No. 11975187, and the Natural Science Foundation of ChongQing under Grant No. CSTB2023 NSCQ-MSX0132. The work of F. F. is supported by the National Natural Science Foundation of China under Grant No. 12275353. This work is supported in part by the Natural Science Foundation of China under Grant No. 11847301 and by the Fundamental Research Funds for the Central Universities under Grant No. 2019CDJDWL0005.

APPENDIX A: CONSTRUCTION OF HELICITY PROJECTORS

In this appendix, we present the helicity projectors $\mathcal{P}^{(H)}_{\lambda_1,\lambda_2}$, which have been used to compute the helicity amplitudes for $\eta_b(\chi_{bJ}) \to J/\psi J/\psi$ in Sec. IV. We apply the similar technique applied in [5,20].

For convenience, we introduce an auxiliary transverse metric tensor and two auxiliary longitudinal vectors,

$$g_\perp^{\mu\nu} = g^{\mu\nu} + \frac{P^\mu P^\nu}{|\mathbf{P}|^2} - \frac{Q\cdot P}{m_H^2|\mathbf{P}|^2}(P^\mu Q^\nu + Q^\mu P^\nu) + \frac{m_{J/\psi}^2}{m_H^2|\mathbf{P}|^2}(Q^\mu Q^\nu), \tag{A1a}$$

$$L_H^\mu = \frac{1}{|\mathbf{P}|}\left(P^\mu - \frac{Q\cdot P}{m_H}Q^\mu\right), \tag{A1b}$$

$$L_{J/\psi}^\mu = \frac{1}{|\mathbf{P}|}\left(\frac{P\cdot Q}{m_H m_{J/\psi}}P^\mu - \frac{m_{J/\psi}}{m_H}Q^\mu\right), \tag{A1c}$$

where P and Q denote the momenta of J/ψ and H, respectively. It is obvious that the transverse metric tensor satisfies the properties

$$g_{\perp\mu\nu}P^\mu = g_{\perp\mu\nu}Q^\mu = 0, \tag{A2a}$$

$$g_{\perp\mu}^\mu = 2, \tag{A2b}$$

$$g_{\perp\mu\alpha}g_\perp^{\alpha\nu} = g_{\perp\mu\alpha}g^{\alpha\nu} = g_{\perp\mu}^\nu. \tag{A2c}$$

The longitudinal vectors satisfy $L_H^\mu Q_\mu = L_{J/\psi}^\mu P_\mu = 0$.

We enumerate all eight helicity projectors:

$$\mathcal{P}_{1,1}^{(\eta_b)\mu\nu} = \frac{i}{2m_{\eta_b}|\mathbf{P}|}\epsilon^{\mu\nu\rho\sigma}Q_\rho P_\sigma, \tag{A3a}$$

$$\mathcal{P}_{1,1}^{(\chi_{b0})\mu\nu} = -\frac{1}{2}g_\perp^{\mu\nu}, \tag{A3b}$$

$$\mathcal{P}_{0,0}^{(\chi_{b0})\mu\nu} = L_{J/\psi}^\mu L_{J/\psi}^\nu, \tag{A3c}$$

$$\mathcal{P}_{1,0}^{(\chi_{b1})\mu\nu\alpha} = \frac{-1}{2m_{\chi_{b1}}|\mathbf{P}|}\epsilon^{\mu\nu\rho\sigma}Q_\rho P_\sigma L_{J/\psi}^\alpha, \tag{A3d}$$

$$\mathcal{P}^{(\chi_{b2})\mu\nu\alpha\beta}_{1,-1} = \frac{1}{4}(g^{\mu\nu}_{\perp} g^{\alpha\beta}_{\perp} - g^{\mu\alpha}_{\perp} g^{\nu\beta}_{\perp} - g^{\mu\beta}_{\perp} g^{\nu\alpha}_{\perp}), \tag{A3e}$$

$$\mathcal{P}^{(\chi_{b2})\mu\nu\alpha\beta}_{1,1} = \frac{-1}{2\sqrt{6}}(g^{\mu\nu}_{\perp} + 2L^{\mu}_{H} L^{\nu}_{H}) g^{\alpha\beta}_{\perp}, \tag{A3f}$$

$$\mathcal{P}^{(\chi_{b2})\mu\nu\alpha\beta}_{1,0} = \frac{-1}{2\sqrt{2}}(g^{\mu\alpha}_{\perp} L^{\nu}_{H} + g^{\nu\alpha}_{\perp} L^{\mu}_{H}) L^{\beta}_{J/\psi}, \tag{A3g}$$

$$\mathcal{P}^{(\chi_{b2})\mu\nu\alpha\beta}_{0,0} = \frac{1}{\sqrt{6}}(g^{\mu\nu}_{\perp} + 2L^{\mu}_{H} L^{\nu}_{H}) L^{\alpha}_{J/\psi} L^{\beta}_{J/\psi}. \tag{A3h}$$

If we express the decay amplitudes of $\eta_b(\chi_{bJ}) \to J/\psi(\lambda_1) J/\psi(\lambda_2)$ as

$$\mathcal{A}^{(\eta_b)} = \mathcal{A}^{(\eta_b)}_{\mu\nu} \epsilon^{*\mu}_{J/\psi}(\lambda_1) \epsilon^{*\nu}_{J/\psi}(\lambda_2), \tag{A4a}$$

$$\mathcal{A}^{(\chi_{b0})} = \mathcal{A}^{(\chi_{b0})}_{\mu\nu} \epsilon^{*\mu}_{J/\psi}(\lambda_1) \epsilon^{*\nu}_{J/\psi}(\lambda_2), \tag{A4b}$$

$$\mathcal{A}^{(\chi_{b1})} = \mathcal{A}^{(\chi_{b1})}_{\mu\nu\alpha} \epsilon^{\mu}_{\chi_{b1}} \epsilon^{*\nu}_{J/\psi}(\lambda_1) \epsilon^{*\alpha}_{J/\psi}(\lambda_2), \tag{A4c}$$

$$\mathcal{A}^{(\chi_{b2})} = \mathcal{A}^{(\chi_{b2})}_{\mu\nu\alpha\beta} \epsilon^{\mu\nu}_{\chi_{b2}} \epsilon^{*\alpha}_{J/\psi}(\lambda_1) \epsilon^{*\beta}_{J/\psi}(\lambda_2), \tag{A4d}$$

where $\epsilon_{J/\psi}$, $\epsilon_{\chi_{b1}}$, and $\epsilon_{\chi_{b2}}$ represent the polarization vector/tensor of J/ψ, χ_{b1}, and χ_{b2}, respectively, the helicity amplitude can be computed through

$$\mathcal{A}^{(\eta_b)}_{1,1} = \mathcal{P}^{(\eta_b)\mu\nu}_{1,1} \mathcal{A}^{(\eta_b)}_{\mu\nu}, \tag{A5a}$$

$$\mathcal{A}^{(\chi_{b0})}_{1,1} = \mathcal{P}^{(\chi_{b0})\mu\nu}_{1,1} \mathcal{A}^{(\chi_{b0})}_{\mu\nu}, \tag{A5b}$$

$$\mathcal{A}^{(\chi_{b0})}_{0,0} = \mathcal{P}^{(\chi_{b0})\mu\nu}_{0,0} \mathcal{A}^{(\chi_{b0})}_{\mu\nu}, \tag{A5c}$$

$$\mathcal{A}^{(\chi_{b1})}_{1,0} = \mathcal{P}^{(\chi_{b1})\mu\nu\alpha}_{1,0} \mathcal{A}^{(\chi_{b1})}_{\mu\nu\alpha}, \tag{A5d}$$

$$\mathcal{A}^{(\chi_{b2})}_{1,-1} = \mathcal{P}^{(\chi_{b2})\mu\nu\alpha\beta}_{1,-1} \mathcal{A}^{(\chi_{b2})}_{\mu\nu\alpha\beta}, \tag{A5e}$$

$$\mathcal{A}^{(\chi_{b2})}_{1,1} = \mathcal{P}^{(\chi_{b2})\mu\nu\alpha\beta}_{1,1} \mathcal{A}^{(\chi_{b2})}_{\mu\nu\alpha\beta}, \tag{A5f}$$

$$\mathcal{A}^{(\chi_{b2})}_{1,0} = \mathcal{P}^{(\chi_{b2})\mu\nu\alpha\beta}_{1,0} \mathcal{A}^{(\chi_{b2})}_{\mu\nu\alpha\beta}, \tag{A5g}$$

$$\mathcal{A}^{(\chi_{b2})}_{0,0} = \mathcal{P}^{(\chi_{b2})\mu\nu\alpha\beta}_{0,0} \mathcal{A}^{(\chi_{b2})}_{\mu\nu\alpha\beta}. \tag{A5h}$$

APPENDIX B: DECAY WIDTHS AND BRANCHING RATIOS FOR DIFFERENT r

By fixing LDMEs, $\mu_R = m_b$ and $m_b = 4.7$ GeV, and varying m_c from 1.25 GeV to 1.9 GeV, we tabulate the decay widths and branching fractions in Table IV. The branching fraction as a function of r has been illustrated in Fig. 3.

TABLE IV. Theoretical predictions on various unpolarized decay widths (in units of eV) and branching fractions ($\times 10^{-5}$).

	r	0.267		0.286		0.308		0.333		0.364		0.400	
H	Order	Γ	Br	Γ	Br	Γ	Br	Γ	Br	Γ	Br	Γ	Br
η_b	LO	...	...	...	...	...	...	...	...	...	...	...	...
	NLO	2.407	0.024	2.341	0.023	2.231	0.022	2.059	0.021	1.796	0.018	1.401	0.014
	NNLO	9.245	0.092	8.944	0.089	8.468	0.085	7.749	0.077	6.688	0.067	5.151	0.052
χ_{b0}	LO	14.978	1.309	12.664	1.107	10.563	0.923	8.690	0.760	7.065	0.618	5.722	0.500
	NLO	21.144	1.848	17.267	1.509	13.826	1.209	10.831	0.947	8.299	0.725	6.250	0.546
	NNLO	12.177	1.064	9.951	0.870	7.956	0.695	6.202	0.542	4.708	0.412	3.502	0.306
χ_{b1}	LO	...	...	...	...	...	...	...	...	...	...	...	...
	NLO	0.044	0.055	0.037	0.047	0.031	0.039	0.024	0.030	0.016	0.021	0.009	0.012
	NNLO	0.099	0.125	0.082	0.104	0.065	0.082	0.048	0.061	0.032	0.040	0.017	0.022
χ_{b2}	LO	33.173	18.848	30.015	17.054	27.096	15.396	24.423	13.877	22.002	12.501	19.848	11.277
	NLO	13.545	7.696	11.845	6.730	10.253	5.825	8.764	4.979	7.370	4.187	6.058	3.442
	NNLO	0.410	0.233	0.438	0.249	0.459	0.261	0.472	0.268	0.473	0.269	0.458	0.260

[1] G. T. Bodwin, E. Braaten, and G. P. Lepage, Phys. Rev. D **51**, 1125 (1995); **55**, 5853(E) (1997).
[2] S. D. Yang *et al.* (Belle Collaboration), Phys. Rev. D **90**, 112008 (2014).
[3] C. P. Shen *et al.* (Belle Collaboration), Phys. Rev. D **85**, 071102 (2012).
[4] Y. Jia, Phys. Rev. D **76**, 074007 (2007).
[5] J. Xu, H. R. Dong, F. Feng, Y. J. Gao, and Y. Jia, Phys. Rev. D **87**, 094004 (2013).
[6] W. L. Sang, F. Feng, and Y. Q. Chen, Phys. Rev. D **92**, 014025 (2015).
[7] Y. D. Zhang, W. L. Sang, and H. F. Zhang, Phys. Rev. Lett. **129**, 112002 (2022).
[8] Y. Jia, Phys. Rev. D **78**, 054003 (2008).
[9] B. Gong, Y. Jia, and J. X. Wang, Phys. Lett. B **670**, 350 (2009).
[10] V. V. Braguta and V. G. Kartvelishvili, Phys. Rev. D **81**, 014012 (2010).
[11] P. Sun, G. Hao, and C. F. Qiao, Phys. Lett. B **702**, 49 (2011).
[12] V. V. Braguta, A. K. Likhoded, and A. V. Luchinsky, Phys. At. Nucl. **73**, 1054 (2010).
[13] J. Zhang, H. Dong, and F. Feng, Phys. Rev. D **84**, 094031 (2011).
[14] W. L. Sang, R. Rashidin, U. R. Kim, and J. Lee, Phys. Rev. D **84**, 074026 (2011).
[15] L. B. Chen and C. F. Qiao, Phys. Rev. D **89**, 074004 (2014).
[16] F. Feng, Y. Jia, Z. Mo, W. L. Sang, and J. Y. Zhang, arXiv: 1901.08447.
[17] X. D. Huang, B. Gong, and J. X. Wang, J. High Energy Phys. 02 (2023) 049.
[18] W. L. Sang, F. Feng, Y. Jia, Z. Mo, and J. Y. Zhang, Phys. Lett. B **843**, 138057 (2023).
[19] W. L. Sang, F. Feng, Y. Jia, Z. Mo, J. Pan, and J. Y. Zhang, Phys. Rev. Lett. **131**, 161904 (2023).
[20] Y. D. Zhang, F. Feng, W. L. Sang, and H. F. Zhang, J. High Energy Phys. 12 (2021) 189.
[21] H. E. Haber, arXiv:hep-ph/9405376.
[22] M. Jacob and G. C. Wick, Ann. Phys. (N.Y.) **7**, 404 (1959).
[23] V. L. Chernyak and A. R. Zhitnitsky, Sov. J. Nucl. Phys. **31**, 544 (1980).
[24] S. J. Brodsky and G. P. Lepage, Phys. Rev. D **24**, 2848 (1981).
[25] A. Czarnecki and K. Melnikov, Phys. Rev. Lett. **80**, 2531 (1998).
[26] M. Beneke, A. Signer, and V. A. Smirnov, Phys. Rev. Lett. **80**, 2535 (1998).
[27] A. Czarnecki and K. Melnikov, Phys. Lett. B **519**, 212 (2001).
[28] A. H. Hoang and P. Ruiz-Femenia, Phys. Rev. D **74**, 114016 (2006).
[29] W. L. Sang, F. Feng, Y. Jia, and S. R. Liang, Phys. Rev. D **94**, 111501 (2016).
[30] W. L. Sang, F. Feng, and Y. Jia, J. High Energy Phys. 10 (2020) 098.
[31] T. Hahn, Comput. Phys. Commun. **140**, 418 (2001).
[32] V. Shtabovenko, R. Mertig, and F. Orellana, Comput. Phys. Commun. **207**, 432 (2016).
[33] F. Feng and R. Mertig, arXiv:1212.3522.
[34] M. Beneke and V. A. Smirnov, Nucl. Phys. **B522**, 321 (1998).
[35] F. Feng, Comput. Phys. Commun. **183**, 2158 (2012).
[36] A. V. Smirnov, Comput. Phys. Commun. **189**, 182 (2015).
[37] H. H. Patel, Comput. Phys. Commun. **197**, 276 (2015).
[38] X. Liu, Y. Q. Ma, and C. Y. Wang, Phys. Lett. B **779**, 353 (2018).
[39] Z. F. Liu and Y. Q. Ma, Phys. Rev. Lett. **129**, 222001 (2022).
[40] X. Liu and Y. Q. Ma, Comput. Phys. Commun. **283**, 108565 (2023).
[41] X. Liu and Y. Q. Ma, Phys. Rev. D **105**, 5 (2022).
[42] https://gitlab.com/multiloop-pku/calcloop.
[43] D. J. Broadhurst, N. Gray, and K. Schilcher, Z. Phys. C **52**, 111 (1991).
[44] P. A. Zyla *et al.* (Particle Data Group Collaboration), Prog. Theor. Exp. Phys. **2020**, 083C01 (2020).
[45] E. J. Eichten and C. Quigg, Phys. Rev. D **52**, 1726 (1995).
[46] K. G. Chetyrkin, J. H. Kuhn, and M. Steinhauser, Comput. Phys. Commun. **133**, 43 (2000).
[47] N. Brambilla *et al.* (Quarkonium Working Group Collaboration), Heavy quarkonium physics, 10.5170/CERN-2005-005.
[48] L. B. Chen and C. F. Qiao, J. High Energy Phys. 11 (2012) 168.
[49] V. V. Braguta, A. K. Likhoded, and A. V. Luchinsky, Phys. Rev. D **72**, 094018 (2005).